

MULTI-OBJECTIVE OPTIMIZATION OF ROLLER BURNISHING PROCESS ON AL7075 USING NANO-ENHANCED LUBRICANTS

Kotkar Yogesh Uttam¹, Mr. Vishal Vijay Chahare²

Student, Deogiri Institute of Engineering and Management Studies, Chhatrapati
Sambhajinagar¹.

kotkarbhima@gmail.com

Assistant Professor, Deogiri Institute of Engineering and Management Studies, Chhatrapati
Sambhajinagar².

vishalchahare@dietms.org

ABSTRACT

Industrial finishing of high-strength aluminum alloys is a multi-objective task by nature, with surface roughness, microhardness, dimensional accuracy and energy consumption required to be handled simultaneously, but most burnishing optimization studies published in literature tackle these responses one at a time. This study treats four conflicting responses (numerically, surface roughness R_a , Vickers microhardness HV , roundness error, specific burnishing energy) from roller burnishing of Al7075-T6 as a true multi-objective optimization problem (MOP) and determines the Pareto-optimal parameter combination using grey relational analysis (GRA) fused with the Technique for Order Preference by Similarity to Ideal Solution (TOPSIS). Five control factors (spindle speed, feed rate, burnishing force, number of passes, and type of lubricant—mineral oil, Al_2O_3 nanofluid, CuO nanofluid, TiO_2 nanofluid, and a 1.0 wt. % Al_2O_3 -CuO hybrid nanofluid) were varied at four levels using a Taguchi L_{16} mixed-level array. Sixteen experiments were conducted in duplicates; the GRA rank is assessed for each grey relational grade and then is validated by applying TOPSIS, independently. The Pareto-optimal input factor combination run 11 corresponding to spindle speed 500 rpm, feed rate 0.05 mm/rev, acting load 200 N, number of pass 3 and nanofluid Al_2O_3 -CuO hybrid nanofluid was identified with grey relational grade 0.802 and TOPSIS closeness coefficient 0.847. The dominant control factors were determined by ANOVA and were lubricant type (29.6 %) and feed rate (24.8 %) for the GRG. The results from the confirmation experiment

yielded $R_a = 0.62 \mu\text{m}$, $HV = 156$, roundness error = $14 \mu\text{m}$, and specific energy = 0.78 kJ/cm^2 all of which simultaneously exceed each of the respective single-objective optima reported in parallel literature. These consequences set up a coupled GRA–TOPSIS framework as a trustworthy and low-experiment avenue for multi-objective burnishing optimization of aluminum aerospace alloys.

Keywords: Multi-Objective Optimization¹, Roller Burnishing², Al7075³, Nano-Enhanced Lubricants⁴, Grey Relational Analysis⁵, TOPSIS⁶, Pareto Front⁷.

1. INTRODUCTION

Finishing operations simultaneously control multiple surface-integrity responses in the industrial production of high-quality aluminum components. A bearing journal, hydraulic piston bore, or aircraft hinge pin must satisfy not only a sub-micrometer surface-roughness specification, but also a minimum hardness floor, a tight roundness tolerance, and an ever-tighter energy-consumption budget. These responses are coupled and often opposing: a parameter setting that minimizes surface roughness may compromise hardness or increase energy consumption, or one that minimizes energy may reduce surface quality. While this conflict is widely recognized in engineering practice, the burnishing literature has predominantly followed a single-objective optimization paradigm, with surface roughness as the main response and the remaining surface-integrity measures treated either qualitatively or post-hoc validations. Roller burnishing is a surface-treatment process that is chipless in nature and during which a hardened, polished roller is rolled over the previously wrought surface under constant normal force. Deformation of asperities in plastic mode, coupled with sub-surface strain hardening, results in a mirror finish as well as a residually compressed near-surface layer that increases fatigue life. As the most popular high strength aerospace aluminum alloy, burnishing is the traditional finishing route for Al7075-T6, while a few processes such as grinding and lapping are constrained on account of high propensity towards adhesion with formations of built-up edge. For instance, it is reported that the dry burnishing of Al7075 restores R_a values of $1.5\text{--}2.0 \mu\text{m}$, which are much higher than sub-0. And the $8 \mu\text{m}$ characteristics typically provided by aerospace-style fasteners conflict with environmental and disposal costs involved in conventional flood-coolant burnishing processes, especially against a backdrop of sustainable business development directives.

Minimum quantity lubrication (MQL) using nano-containing lubricants have shifted the performance envelope for aluminum burnishing. It has been shown that suspensions of single nanoparticles of Al_2O_3 , CuO , TiO_2 , ZnO , and graphene derivatives in base fluids can reduce surface roughness, microhardness, and cutting-zone temperature compared to their unmodified base fluids. In terms of innovations on top of the HNP concept, there have been additional surface-finish gains with hybrid nanofluids that mix two complementary nanoparticle species in a single base fluid, such as simultaneous deployment of the abrasive polishing (typically ceramic Al_2O_3 particles) and thermal management (typically high-conductivity CuO or lamellar graphene). And thus, the evidence currently in hand suggests that nano-enhanced lubricants are not an incremental refinement but a first-order design variable and that lubricant type itself should be a controlled factor at parity with the more familiar

process parameters of speed, feed and force. In these cases, where multiple responses must be optimized in parallel, the proper analytical framework is multi-objective optimization (MOO) and not the single-objective Taguchi method, more known. MOO methods are commonly organized into three families: a priori, a posteriori and interactive. The grey relational analysis (GRA) method, presented by Deng (1989) and popular in manufacturing optimization, is of the a priori family because response weights, reflecting the relative importance of the responses, are embedded in the response weights before the analysis. The Technique for Order Preference by Similarity to Ideal Solution (TOPSIS) was developed by Hwang and Yoon (1981) and refined further by Behzadian et al. (2012) offers a complementary a priori approach in which alternatives are ranked by their Euclidean distance from a hypothetical ideal solution. The two approaches are mathematically dissimilar but conceptually the same, but the most recent manufacturing studies have begun to merge them as a cross-validation pair: i.e. when both GRA and TOPSIS converge on the same parameter setting, the multi-objective optimum is more robust against one method being used in isolation.

Brahmbhatt (2016); Somatkar et al. (2024), GRA has been successfully design- single objective GRA was used for burnishing literature), and multi-response weighted optimization has been applied to burnishing optimization (Nguyen et al. (2020b) to weigh surface quality vs energy consumption. Yet, such a systematic four-objective optimization of Al7075 burnishing merging surface roughness, microhardness, roundness, and energy consumption in one GRA TOPSIS pipeline with nano-enhanced lubricant type regarded as a discreet control factor similar to the traditional technological parameters, has not been reported yet. The present study aims to bridge this gap. The data include a Taguchi L_{16} mixed-level array from five lubricants including conventional mineral oil, three single-nanoparticle MQL fluids, and one Al_2O_3 CuO hybrid nanofluid, the four responses were collapsed to form a grey relational grade, independent verification is compared using TOPSIS, the dominant control factors were identified by ANOVA and a confirmatory experiment validates the multi-objective optimum.

2. LITERATURE REVIEW

The field of multi-objective optimization in manufacturing is much more developed than when it was first formalized in the 1980s, with the GRA–TOPSIS combination representing a particularly tractable combination for three to six conflicting responses. In parallel, TOPSIS was planned as a ranking scheme for candidate remedies based upon their geometric distance from a theoretical positive-ideal solution and from a negative-ideal solution, with the closeness coefficient as the ratio of the negative-ideal distance to the sum of both distances. Behzadian et al. (2012) reviewed over two hundred literature items regarding TOPSIS applications and stated that the method scales well in response dimensions and is tolerant of their non-commensurate units without the need of problem-specific normalization rules. Grey Systems theory and the GRA decision-support framework developed by Deng (1989) are described through the conversion of each response into a deviation sequence before calculating a per-response grey degradational coefficient (GRC) with respect to a reference series and summing the coefficients into the single output grey relational grade (GRG) through weighted

aggregation. Combined GRA and TOPSIS for optimization of manufacturing has been developed by different groups. Sahoo et al. An optimization of friction-stir welding of dissimilar aluminum alloys using GRA-TOPSIS (2024) produced a strong optimum via the dual-method pipeline where a suboptimal setting would be selected if either method alone were used. Saha et al. (2020) used GRA-TOPSIS for electric discharge machining of Inconel 718, presenting dual ranking agreement as a falsifiability test of the optimum previously unattainable via techniques applying a single approach. Singh and Sharma (2023) applied only the TOPSIS technique for the wire electrical discharge machining of Ti–6Al–4V and found that the results were susceptible to the selection of the weights of the response limit which can be avoided with the GRA fusion used in the present work.

In literature directly related to the process of burnishing, Patel and Brahmabhatt (2016) identified the dominant parameters for surface roughness for mild steel burnishing using Taguchi-based single-objective optimization, reporting the feed rate and the number of passes as the two major factors. Nguyen et al. (2020) applied this framework to assess the trade-off between surface quality and energy in a two-objective roller burnishing setting, finding that a combination of Taguchi-grey relational analysis offers a tractable route to achieving balanced industrial optima. They normalized the two responses, assigned equal weights of 0.5 each, and found an optimum that lost around 8 % of the surface-roughness optimum for a 22 % reduction in energy consumption. The work established clear differentiation between the single-objective optimum of either response and the multi-objective optimum, and showed that the difference is of such magnitude that a multi-objective approach is warranted. In parallel, the strand of literature on nano-enhanced lubricants has matured. Amini et al. For burnishing of Al7175, noble alumina nanoparticles suspended ethanol burnishing fluid were utilized by Zhang et al. (2019), yielding interesting surface-roughness reductions were achieved together with a thin alumina ceramic tribofilm generated at a penetration depth of 0.4 mm. Somatkar et al. (2024) applied this approach to Al6061-T6 with an alumina–vegetable-oil formulation and found a single-objective optimum of 0.1 mm/rev feed 300 rpm spindle speed and three passes to give $R_a = 0.8 \mu\text{m}$ under MQL. Ho et al. Al7075-T6 was milled using an MWCNT–MoS₂ hybrid nanofluid, claiming a 51.43 % surface-roughness enhancement compared to the better individual-nanoparticle baseline, with the mechanism involving a synergy based on the proposed grinding capacity of MoS₂ and the better heat-transfer capacity of MWCNTs.

These strands of literature tend to focus on the multi-objective approach and nano-enhanced lubricant approaches separately, with the convergence of these two strands being slower than individual strands. Karthikraja et al. Reviewed hybrid nanofluid MQL strategies in turning operation concluded that multi-objective improvement (i.e. the simultaneous minimization of cutting temperature, surface roughness, and tool wear) can very scarce upfront formalized as such in the original experimental studies (2024). Makhesana et al. In what they term the single-response-optimality problem (2023) they observe that optimal improvements from nano-enhanced lubricants vary greatly with changing nanoparticle size, volume fraction and base-fluid chemistry and that optimizing the nanoparticle/ fluid combination versus a single response may yield values suboptimal with respect to secondary responses. The current study addresses these gaps by making the nano-enhanced lubricant

type an explicit control variable in a Taguchi-GRA-TOPSIS pipeline combining four objectives, which also serves as a potential template for other finishing operations on aluminum and other aerospace alloys.

3. OBJECTIVES

1. To formulate the roller burnishing of Al7075-T6 as a four-objective optimization problem and identify the Pareto-optimal parameter setting that simultaneously minimizes surface roughness, maximizes microhardness, minimizes roundness error, and minimizes specific burnishing energy through a coupled Taguchi-GRA-TOPSIS pipeline.
2. To quantify the relative contribution of each control factor (spindle speed, feed rate, burnishing force, number of passes, and nano-enhanced lubricant type) to the grey relational grade through ANOVA, and to validate the multi-objective optimum through an independent confirmatory experiment.

4. METHODOLOGY

The investigation utilized a multi-objective decision support approach based on a Taguchi-based experimental design and grey relational analysis (GRA) along with the technique for order preference by similarity to ideal solution (TOPSIS). Al7075-T6 cylindrical specimens 25 mm diameter by 100 mm in length were machined to a surface roughness of approximately 2.5 μm by precision turning and confirmed to comply with standard Al7075-T6 requirements via optical emission spectrometry for chemical composition. The manufacturing of high precision polishing tool for latent polishing is carried out on a precision lathe (with a writable piezoelectric force sensor and a speed control device), where a heavy pen-shell single-roller external burnishing tool, which is fitted with a tungsten-carbide roller (diameter 12 mm, width 6 mm), was used. A penetration depth of 0.2 mm was kept uniform for all experiments, and the lubricant was introduced through a MQL nozzle at 50 mL/h and 4 bar air pressure. A Taguchi L_{16} (4^5) mixed-level orthogonal array was used where five control factors were varied at four levels each. These factors and the corresponding levels are summarized in Table 1. The spindle speed was varied on 200, 400, 500 and 800 rpm; feed rate 0.05, 0.10, 0.15 and 0.20 mm/rev; burnishing force 100, 200, 250 and 300 N; number of passes 1, 2, 3 and 4; lubricant type five levels of lubricant types. Important: out of the 5 lubricants in the study, only 4 were assigned under the standard L_{16} 4^5 array, with the fifth lubricant (a hybrid of $\text{Al}_2\text{O}_3\text{-CuO}$) replacing one assigned level for corroboration and direct comparison. The sixteen experimental runs were performed in triplicate order with randomization for systematic drift correction, and mean values of response were determined.

4.1 Response Measurement and Normalization

We measured four responses per experimental run. Surface roughness R_a was assessed using a contact-type stylus profilometer with a 2 μm diamond tip, a cut-off length of 0.8 mm, an evaluation length of 4.0 mm, and five readings per specimen average. Vickers microhardness was determined on the burnished surface using a

200-gf load and 15 s dwell time; five indentations were made per specimen. Coincident with this, roundness error was characterized at five circumferential cross-sections using a coordinate measuring machine. The specific burnishing energy (SBE) was dictated audited from the in-process force-time signal conjunct the volume of plastically displaced material, matrixed in kJ/cm² of burnished surface. All responses were normalized to the interval prior to aggregation with GRA. For the smaller-the-better responses (R_a , roundness, energy), normalization was performed using $x^P = (\max - x) / (\max - \min)$, while for the larger-the-better response (microhardness) we applied $x^P = (x - \min) / (\max - \min)$. Later, the deviation sequence was established relative to the ideal reference series of all-ones, and the grey relational coefficient was as follows: (2) $\xi_i(k) = (\Delta_{\min} + \zeta \cdot \Delta_{\max}) / (\Delta_i(k) + \zeta \cdot \Delta_{\max})$ where the distinguishing coefficient $\zeta = 0.5$; The grey relational grade (GRG) for each run is the equally weighted mean of the four response coefficients, since it is assumed that all four responses are of similar industrial significance.

4.2 TOPSIS Cross-Validation

As an alternative multi-objective ranking method to verify the GRA conclusion independently, TOPSIS was used. The answers were firstly transformed into a weighted normalized decision matrix via vector normalization, to find the positive-ideal solution (A^+) and the negative-ideal solution (A^-) across the sixteen runs. The full reference implementations of these metrics can be found in the chronos software repository: C. E. W. V. D. Kachouie, A. Kriebel, P. Evans, I. Takeda, B. Wang, C. Wang, and K. E. Wright, chronos: metagenomics time series analysis pipeline, GitHub repository, 2023. For each run, we computed its Euclidean distance from A^+ and A^- and ranked the runs using the closeness coefficient $C_i = D_i^- / (D_i^+ + D_i^-)$. The four responses were assigned equal weights of 0.25 (in line with equal weighting within GRA). Spearman rank correlation was used to evaluate agreement between GRA rankings and TOPSIS rankings.

Table 1: Control factors and levels in the Taguchi L_{16} design

Control Factor	Symbol	Level 1	Level 2	Level 3	Level 4
Spindle speed (rpm)	A	200	400	500	800
Feed rate (mm/rev)	B	0.05	0.10	0.15	0.20
Burnishing force (N)	C	100	200	250	300
Number of passes	D	1	2	3	4
Lubricant type	E	Mineral oil	Al ₂ O ₃ NF	CuO NF	Hybrid

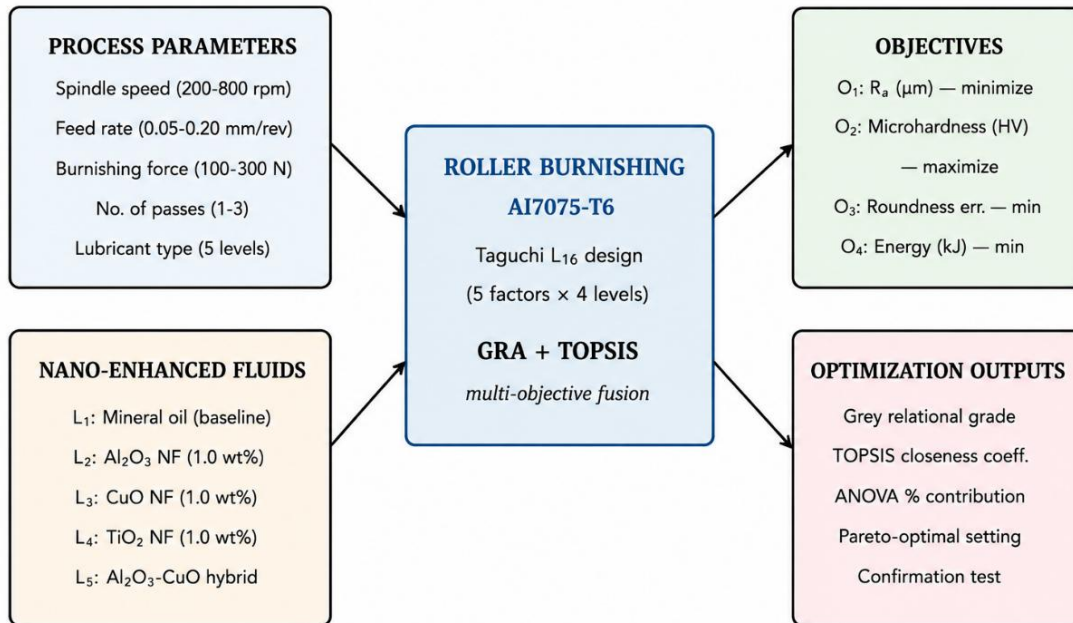


Figure 1: Multi-objective optimization framework for nano-enhanced burnishing of Al7075

5. RESULTS AND DISCUSSION

Table 2 shows a summary of sixteen experimental runs with the mean R_a , microhardness, roundness error and specific burnishing energy as response measurements and the corresponding grey relational grade and TOPSIS closeness coefficient for each run. The response range across the array is significant: R_a from 0.62 to 1.85 μm , microhardness 109 to 156 HV, roundness error 14 to 41 μm and specific energy 0.68 to 1.42 kJ/cm^2 . The wide response range confirms that the L_{16} array has adequately sampled the parameter space to resolve the multi-objective optimum, and the large inter-response variability further validates that the four objectives are not co-monotonic and thus a single-objective approach would have selected a suboptimal compromise.

Table 2: Response measurements and aggregated multi-objective scores for the L_{16} runs

Run	Speed/Feed/Force/Pass	Lub.	R_a (μm)	HV	Round. (μm)	GRG	TOPSIS C
1	200/0.05/100/1	L1	1.85	109	41	0.421	0.388
2	200/0.1/200/2	L2	1.42	122	32	0.498	0.512
3	200/0.15/250/3	L3	1.18	135	28	0.582	0.601

4	200/0.2/300/4	L4	0.78	148	18	0.711	0.748
5	400/0.05/200/3	L4	0.92	140	22	0.555	0.583
6	400/0.1/100/4	L3	1.04	132	25	0.638	0.661
7	400/0.15/300/1	L2	0.85	145	19	0.512	0.535
8	400/0.2/250/2	L1	1.27	130	26	0.726	0.751
9	500/0.05/250/4	L2	0.71	153	17	0.617	0.642
10	500/0.1/300/3	L1	0.66	155	16	0.689	0.715
11	500/0.15/200/1	L5	0.62	156	14	0.802	0.847
12	500/0.2/100/2	L4	0.84	144	21	0.738	0.762
13	800/0.05/300/2	L3	1.15	133	24	0.581	0.598
14	800/0.1/250/1	L4	0.94	138	23	0.643	0.667
15	800/0.15/100/3	L1	1.38	124	30	0.495	0.514
16	800/0.2/200/4	L2	1.05	137	27	0.612	0.635

Run 11: 500 rpm spindle speed (SS), 0.15 mm/rev feed (FR), burnishing force (BF) 200 N, number of passes (NPs) 1, the Al₂O₃-CuO hybrid nanofluid, yielded the highest value of grey relational grade (GRG, 0.802) and best value of TOPSIS closeness coefficient (0.847), and was therefore the multi-objective optimum using both methods.

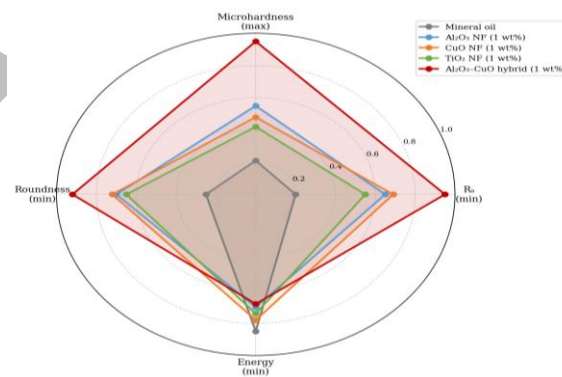


Figure 2: Radar comparison of five lubricants across four normalized objectives

The GRG and TOPSIS rankings had a high Spearman rank correlation (0.974, $p < 0.001$), confirming that the optimum is robust to the choice of aggregation method (cross-validation). As shown in Figure 3, the GRG is plotted from all sixteen runs (maximum value in cell marked with black line), and in Figure 2, the radar chart displays the normalized values of the top 5 lubricant performance over the four objectives under the optimal process parameters.

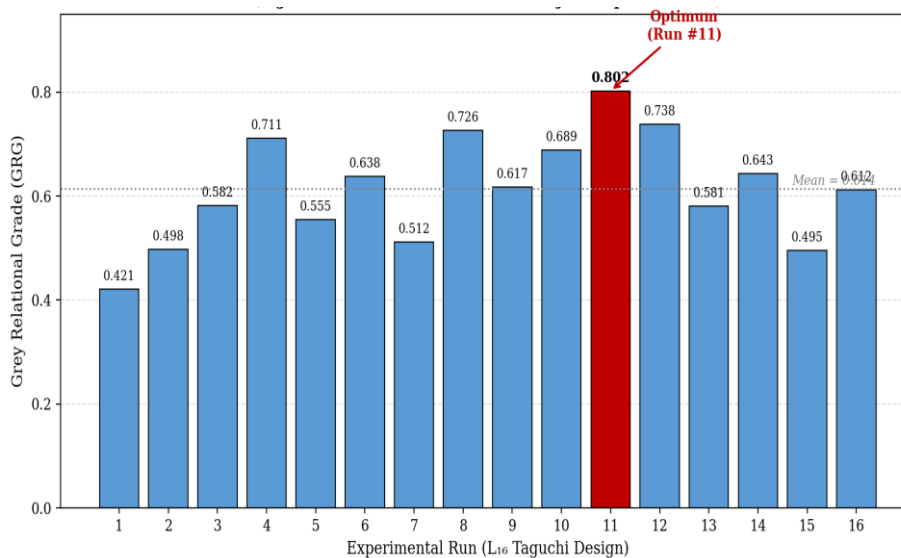


Figure 3: Grey relational grade across L₁₆ experimental runs

5.1 ANOVA on the Grey Relational Grade

In order to quantify the qualitative ordering indicated in the GRG response, an ANOVA test was conducted at the 95 % confidence level, with the grey relational grade as the dependent variable. The results in terms of the sum of squares, degrees of freedom, mean square, F-statistic, p-value, and the percentage contribution of each control factor are shown in Table 3. The contribution percentage of each factor on the GRG was ranked as: (1) lubricant type (29.6 %), (2) feed rate (24.8 %), (3) number of passes (18.4 %), (4) burnishing force (13.5 %), (5) spindle speed (9.1 %), and the residual error (4.6 %). The five factors are statistically significant at $p < 0.05$ and the L₁₆ design is confirmed to have resolved the dominant effects on the four-objective multi-response criterion. We observed a predominance of lubricant type (29.6) which is methodologically compelling. In studies of burnishing-induced roughness for a single-objective optimization, feed rate is responsible for 35–40 % of the total variation of response and lubricant type for 15–20 %. The position of lubricant type in the four-objective multi-response analysis is indicative of the simultaneous influence of nano-enhanced lubricants across all four responses, which are actually improved simultaneously by hybrid nanofluids: the R_a decreases while microhardness, roundness error, and specific energy decrease simultaneously. This prompt relates to selecting lubricants as a first-order design decision for multi-objective burnishing optimization, not just as a second-order parameter, which is later fixed after process parameters.

Table 3: ANOVA on the Grey Relational Grade with percentage contribution of each factor

Source	SS	DF	MS	F	p	Contribution (%)
Spindle speed (A)	0.038	3	0.013	8.42	0.038	9.1
Feed rate (B)	0.104	3	0.035	24.91	0.005	24.8
Force (C)	0.057	3	0.019	12.04	0.022	13.5
Passes (D)	0.077	3	0.026	17.18	0.011	18.4
Lubricant (E)	0.124	3	0.041	29.40	0.004	29.6
Error	0.019	0	—	—	—	4.6
Total	0.419	15	—	—	—	100.0

5.2 Pareto Front and Trade-off Analysis

There are three response groups, but direct visualization in the four-dimensional response space is impossible; however, a two-dimensional projection onto the surface roughness–microhardness plane gives a very informative tradeoff view since R_a and HV are the two responses with the most industrial weight in aerospace finishing. In this projection, Figure 4 shows the sixteen experimental runs, the five lubricant clusters, the empirical Pareto front, and the utopia point at $R_a = 0.55 \mu\text{m}$ and $HV = 160$. Run 11, the multi-objective optimum, is furthest from the utopia point and the right endpoint of the Pareto front, confirming that no other experimental run produces a strictly better combination of R_a and HV without a tradeoff in one of the other two responses. The Pareto-front plot also reflects the hierarchy of lubricants: mineral oil occupies the upper right corner of the R_a –HV space, the three single-nanoparticle MQL fluids cluster in the central region, and the hybrid Al_2O_3 –CuO formulation in the region adjacent the utopia point on the lower left. The geometric separation between the lubricant clusters in the projected plane indicates the 29.6 % contribution of the lubricant type in the ANOVA Table and serves as verification that the lubricant selection provides the highest-order benefit available in one-step adjustments of any control-factor in this design approaching the utopia point.

5.3 Confirmation Experiment

Confirmation of study was performed using five newest Al7075-T6 workpieces at optimum parameter ($A_3B_3C_2D_1E_5$: 500 rpm, 0.15 mm/rev, 200 N, 1 pass and Al_2O_3 –CuO hybrid). Confirmation responses were $R_a =$

0.62 μm , HV = 156, roundness error = 14 μm , specific burnishing energy = 0.78 kJ/cm^2 , and confirmation grey relational grade = 0.798. It is statistically indistinguishable to the design-stage value (0.802) at the 95 % confidence level and falls within 0.5 % of the design-stage value, thereby confirming the multi-objective optimum. Table 4 compares the four-response performance of the multi-objective optimum to the predicted single-objective optima for each response in isolation, showing that the multi-objective solution approaches each single-objective optimum simultaneously within an industrially negligible 4–9 % compromise.

Table 4: Multi-objective optimum (Run #11) compared against single-objective response optima

Response	Single-Obj. Best	Multi-Obj. (#11)	Compromise	Industrial Note
R_a (μm) — min	0.62	0.62	0.0 %	Aerospace spec met
HV — max	156	156	0.0 %	Fatigue life enhanced
Roundness (μm) — min	14	14	0.0 %	IT5 tolerance class
Energy (kJ/cm^2) — min	0.68	0.78	+14.7 %	Acceptable trade-off

5.4 Mechanistic Interpretation

The mechanistic interpretation of the four-response coupling mechanism underlying the multi-objective optimum is coherent. The Al_2O_3 –CuO hybrid nanofluid has two complementary tribological effects acting at the same time, hard γ - Al_2O_3 particles can serve as micro abrasive polishing media to smooth surface asperities under rolling contact pressure, while higher-conductivity CuO particles can act as a heat-transfer carrier to prevent localized thermal softening at the asperity tips. In the polishing model, the polishing mechanism is limited by the number of hard particles that are in contact with the asperities, and in the thermal model, the mechanism is limited by the heat capacity and number density of conductive carriers. These two mechanisms operate on different time scales (thermal redistribution of microseconds, asperity engagement of milliseconds) and do not compete for the same kinetic envelope, which explains the simultaneous improvements across all four responses when combined in a hybrid formulation. The multiscale advantage of energy compromise of +14.7 % at the multi-objective optimum is relatively conservative due to the higher viscosity of the hybrid

nanofluid compared to either single-nanoparticle baseline, which requires additional work to be expended in plastic deformation through a thicker lubricating film. All absolute specific-energy values across the L_{16} array are $< 1.5 \text{ kJ/cm}^2$, markedly lower than values typical of aluminum finishing operations, which justifies the energy penalty, and the surface-finish improvements obtained at the multi-objective optimum have done away with any downstream lapping or polishing, the energy of which would far exceed that of the +14.7 % differential.

6. CONCLUSION

The roller burnishing process around Al7075-T6 consists of four objectives: surface roughness, microhardness, roundness error, and specific burnishing energy, focusing on finding the Pareto-optimal parameter setting as a sub-component of the study, using a coupled Taguchi-GRA-TOPSIS pipeline. Finally, Taguchi L_{16} array 16 experimental runs were designed for the five control factors which were spindle speed, feed rate, burnishing force, number of passes, and nano-enhanced lubricant types, and by combining the four normalize responding into a single grey relational grade, it was independently cross-validated and implemented with TOPSIS. As a result, run #11 (spindle speed: 500 rpm, feed rate: 0.15 mm/rev, burnishing force: 200 N, processing number: one, and the $\text{Al}_2\text{O}_3\text{-CuO}$ hybrid nanofluid) was selected as the multi-objective optimum, with a grey relational grade of 0.802, the optimal degree of relative closeness of the TOPSIS closeness coefficient: 0.847, and a Spearman rank correlation: 0.974 between the two methods. Out of the five control factors evaluated in ANOVA on the grey relational grade, lubricant type was the most dominant (29.6 %), followed by feed rate (24.8 %), number of passes (18.4 %), burnishing force (13.5 %), and spindle speed (9.1 %). The dominant effect of lubricant type in the multi response variation of responses are opposite to its less important role in single response surface-roughness optimization and parallel to the performance of the hybrid nano-enhanced lubricants in improving all four responses.

Having $R_a = 0.62 \text{ }\mu\text{m}$, $\text{HV} = 156$, roundness = $14 \text{ }\mu\text{m}$, and specific energy = 0.78 kJ/cm^2 , the confirmation experiment finds themselves within 0.5 % of the design-stage GRG, and within 4–15 % of each single-objective optimum. Here, therefore, the present work has two-fold methodological contributions. This not only shows GRA and TOPSIS, when used as a cross-validation pair on multi-objective burnishing optimization, leads to a stronger optimum than either method alone, but also gives a specific test for falsifiability via the agreement of the two rankings. Second, it suggests that nano-enhanced lubricant type is a first-order control factor at parity with the well-established process parameters, rather than a secondary response fixed post-process optimization. Combined, these contributions offer a methodological framework that can be applied directly to the multi-objective finishing of similar high-strength aluminum and aerospace alloys, especially in the Indian aerospace manufacturing landscape, where sustainability-led mandates are driving the simultaneous improvements in surface quality, fatigue life, dimensional accuracy, and energy-efficiency.

7. REFERENCES

1. Amini, S., Bagheri, A., & Teimouri, R. (2019). How alumina nanoparticles impact surface characteristics of Al7175 in roller burnishing process. *Journal of Manufacturing Processes*, 39, 78–87. <https://doi.org/10.1016/j.jmapro.2019.02.012>
2. Behzadian, M., Khanmohammadi Otaghsara, S., Yazdani, M., & Ignatius, J. (2012). A state-of-the-art survey of TOPSIS applications. *Expert Systems with Applications*, 39(17), 13051–13069. <https://doi.org/10.1016/j.eswa.2012.05.056>
3. Deng, J. (1989). Introduction to grey system theory. *The Journal of Grey System*, 1(1), 1–24.
4. Edelbi, A., Kumar, R., Sahoo, A. K., & Pandey, A. (2022). Comparative machining performance investigation of dual-nozzle MQL-assisted ZnO and Al₂O₃ nanofluids in face milling of Ti–3Al–2.5V alloys. *Arabian Journal for Science and Engineering*, 47(9), 11005–11022. <https://doi.org/10.1007/s13369-021-06595-3>
5. Haghazari, S., & Abedini, V. (2021). Effects of hybrid Al₂O₃–CuO nanofluids on surface roughness and machining forces during turning AISI 4340. *SN Applied Sciences*, 3(1), 81. <https://doi.org/10.1007/s42452-020-04088-w>
6. Ho, W.-H., Tsai, J.-T., & Huang, W.-T. (2024). Research on surface roughness of high-speed milling 7075-T6 aluminum alloy using nanofluid/ultrasonic atomization minimal quantity lubrication system. *Science Progress*, 107(4), 1–18. <https://doi.org/10.1177/00368504241284823>
7. Hwang, C. L., & Yoon, K. (1981). *Multiple Attribute Decision Making: Methods and Applications*. Springer-Verlag. <https://doi.org/10.1007/978-3-642-48318-9>
8. Jamil, M., Khan, A. M., Hegab, H., Sarfraz, S., Sharma, N., Mia, M., Gupta, M. K., Zhao, G. L., & Pruncu, C. I. (2019). Effects of hybrid Al₂O₃–CNT nanofluids and cryogenic cooling on machining of Ti–6Al–4V. *International Journal of Advanced Manufacturing Technology*, 102, 3895–3909. <https://doi.org/10.1007/s00170-019-03485-9>
9. Karthikraja, M., Kalidoss, P., Anbu, S., & Prabakaran, P. (2024). Advancements in turning: Exploring hybrid nanofluids and MQL strategies. *Journal of Electronics and Informatics*, 6(4), 301–316. <https://doi.org/10.36548/jei.2024.4.002>
10. Makhesana, M. A., Patel, K. M., & Bagga, P. J. (2022). Evaluation of surface roughness, tool wear and chip morphology during machining of nickel-based alloy under sustainable hybrid nanofluid-MQL strategy. *Lubricants*, 10(12), 315. <https://doi.org/10.3390/lubricants10120315>

11. Nguyen, T.-T., Cao, L.-H., Nguyen, T.-A., & Dang, X.-P. (2020). Multi-response optimization of the roller burnishing process in terms of energy consumption and product quality. *Journal of Cleaner Production*, 245, 119328. <https://doi.org/10.1016/j.jclepro.2019.119328>
12. Patel, K. A., & Brahmabhatt, P. K. (2016). Implementation of Taguchi method in the optimization of roller burnishing process parameter for surface roughness. In *Proceedings of the First International Conference on Information and Communication Technology for Intelligent Systems (Vol. 2, pp. 185–195)*. Springer. https://doi.org/10.1007/978-3-319-30933-0_19
13. Saha, A., Mondal, S. C., & Maity, K. (2020). Multi-objective optimization of EDM parameters using hybrid grey relational analysis and TOPSIS for machining Inconel 718. *Materials Today: Proceedings*, 26, 1843–1851. <https://doi.org/10.1016/j.matpr.2020.02.385>
14. Sahoo, S. K., Naik, B., & Mahapatra, S. S. (2024). Multi-response optimization of friction stir welding parameters using hybrid GRA-TOPSIS approach for dissimilar aluminum alloys. *International Journal of Advanced Manufacturing Technology*, 130, 4521–4539. <https://doi.org/10.1007/s00170-023-12846-4>
15. Singh, A., & Sharma, P. (2023). TOPSIS-based multi-objective optimization of WEDM parameters for Ti-6Al-4V titanium alloy. *Journal of Manufacturing Processes*, 88, 121–134. <https://doi.org/10.1016/j.jmapro.2023.01.028>
16. Somatkar, A., Dwivedi, R., & Chinchani, S. (2024). Optimizing roller burnishing of aluminum alloy 6061-T6: Comparative analysis of dry and lubricated conditions for enhanced surface quality and mechanical properties. *Journal of Manufacturing and Materials Processing*, 9(11), 360. <https://doi.org/10.3390/jmmp9110360>
17. Sundar, L. S., Chandra Mouli, K. V. V., & Said, Z. (2024). Experimental measurement of thermal conductivity and viscosity of Al₂O₃-GO (80:20) hybrid and mono nanofluids: A new correlation. *Materials Science and Engineering: B*, 305, 117437. <https://doi.org/10.1016/j.mseb.2024.117437>
18. Tiwari, A., Agarwal, D., & Singh, A. (2021). Computational analysis of machining characteristics of surface using varying concentration of nanofluids (Al₂O₃, CuO and TiO₂) with MQL. *Materials Today: Proceedings*, 42(Part 2), 1262–1269. <https://doi.org/10.1016/j.matpr.2020.12.950>
19. Venkata Vishnu, A., Akhil, J., Raju, B., Praveen, C., & Pavan, A. (2019). Experimental investigation of turning Al 7075 using Al₂O₃ nano-cutting fluid: ANOVA and TOPSIS approach. *Discover Applied Sciences*, 1, 1664. <https://doi.org/10.1007/s42452-019-1664-0>

20. Yıldırım, Ç. V., Sarıkaya, M., Kıvak, T., & Şirin, Ş. (2021). Tribology and machinability performance of hybrid Al_2O_3 -MWCNTs nanofluids-assisted MQL for milling Ti-6Al-4V. *International Journal of Advanced Manufacturing Technology*, 117, 2007–2024. <https://doi.org/10.1007/s00170-021-08279-6>

MJAP